

A Simple Method Using Tracer Gas to Identify the Main Airflow and Contaminant Paths within a Room

C.-A. Roulet¹, R. Compagnon¹, and M. Jakob¹
LESO-PB, EPFL, Lausanne

Abstract

The main airflow and contaminant paths or the spatial distribution of the age of air (or contaminant) in a room are of great interest in estimating ventilation efficiency. A simple measurement method is presented which consists of injecting one or more tracer gases at locations of interest and analysing the concentration at several other locations, carefully chosen for best accuracy.

Response functions can be fitted to these measurements, which are the age of the tracers or of the air or the concentration of the tracers as a function of the location. The salient paths, such as the dead zones, are also determined from these functions.

The paper presents the method, its application and validation in a well controlled test room.

KEY WORDS:

Indoor air, Age of air, Mapping, Contaminant, Measurement, Tracer gas.

Manuscript received: 12 December 1990
Accepted for publication: 12 June 1991

¹ Laboratoire d'Energie Solaire et de Physique du Bâtiment, ITB, Département d'Architecture, Ecole polytechnique fédérale de Lausanne, CH - 1015 Lausanne

List of symbols

\mathbf{A}	vector containing the coefficients a , b_i , b_{ij} ($i = j$) and b_{ii}	
a , b_i , b_{ij}	coefficients in a model	
$C(\mathbf{r}, t)$	concentration of a tracer at location \mathbf{r} and time t	[-]
$C_e(t)$	concentration measured in the exhaust duct	[-]
$C_o(t)$	concentration measured outdoors	[-]
$C_x(t)$	concentration measured at the location x	[-]
$f(\tau)$	probability density function of the age of air particles	[s ⁻¹]
$F(\tau)$	probability function of the age of air particles	[-]
\mathbf{M}	effect matrix, resulting from an experimental design and a model	
n	air change rate	[s ⁻¹] or [h ⁻¹]
\mathbf{r}	vector locating a point in the space	[m]
t	time	[s]
\mathbf{V}	vector containing the measured quantities ($\nu_1, \nu_2, \dots, \nu_n$) at n locations	
V	volume of the room	[m ³]
x_i	coordinates of a measured point ($i = 1$ to 3)	[m]
$\delta\mathbf{A}$, $\delta\mathbf{V}$	errors in the measurements of \mathbf{A} , \mathbf{V} or \mathbf{M} respectively	
$\delta\mathbf{M}$	norm of the matrix \mathbf{M}	
$\ \mathbf{M}\ $	corresponding norm of the vector \mathbf{V}	
$\ \mathbf{V}\ $		

in that direction. Any point in the zone is then located by three numbers included in the interval $[-1, +1]$.

The experimental design can be represented by a rectangular matrix with 3 lines (one for each coordinate) and as many columns as measured points. For example the design:

Point No.	1	2	3	4
x =	1	-1	1	-1
y	1	-1	-1	1
z	1	-1	1	-1

is very well suited to obtain the coefficients of a linear model. This design may be expanded as follows up to 10 locations for a quadratic model:

Point No.	1	2	3	4	5	6	7	8	9	10
x	1	1	1	1	1	0	-1	-1	-1	-1
y	1	1	-1	-1	-1	0	1	1	-1	-1
z	1	-1	1	0	-1	0	1	-1	1	1

which represent the 8 corners of the zone, its centre and the centre of a vertical angle. This design looks elegant, but cannot provide the coefficients, because the resulting system of equations is singular. To elaborate the most efficient design, it is necessary to look at the method used to obtain these coefficients.

Criteria for Location of the Measurement Points

For each point, the model (Equation 1 or 2 or any other model) is applied, replacing the x_i by their values given by the experimental design. A system of equations (one equation for each location) is obtained, and can be written in a matrix notation:

$$\underline{V} = \underline{M} \underline{A} \quad (3)$$

where:

\underline{V} (v_1, v_2, \dots, v_n) is a vector containing the measured quantities at the n locations,

\underline{M} is a matrix, each line of which corresponds to one location. Its first column is

filled with ones and corresponds to a constant in the model. The next 3 columns may contain the coordinates of the locations if the model contains linear terms. The next 3 columns may contain the products of these coordinates two by two (e.g. x_1x_2, x_1x_3, x_2x_3) in the case of interaction terms and, for a quadratic model, the next three columns contain the squares of the coordinates. Other models will produce other matrices.

\underline{A} is a vector containing the coefficients (e.g. a, b_i, b_{ij} ($i \neq j$) and b_{ii}) of the model.

In general, \underline{M} is rectangular and the least square fit procedure is used:

$$\underline{A} = (\underline{M}'\underline{M})^{-1} \underline{M}' \underline{V} \quad (4)$$

where \underline{M}' is the transposed matrix of \underline{M} . This equation is also valid if \underline{M} is a square matrix, but reduces to the simpler equation:

$$\underline{A} = \underline{M}^{-1} \underline{V} \quad (5)$$

A matrix must be inverted and the determinant of this matrix should not be zero, as is the case for the 10-point design shown above! Since this determinant can be calculated before making the experiments, it is a first criterion for the choice of the experimental design.

If there are experimental errors $\delta\underline{V}$ in \underline{V} or $\delta\underline{M}$ in \underline{M} , these errors will propagate through the equations and errors $\delta\underline{A}$ will result in the coefficients in \underline{A} . In the case of complete experiments, that is if Equation 5 is used, it is shown (Bevinton, 1969) that these errors are smaller than:

$$\frac{|\delta\underline{A}|}{|\underline{A}|} \leq \frac{|\underline{M}| \cdot |\underline{M}^{-1}|}{1 - |\delta\underline{M}| \cdot |\underline{M}^{-1}|} \cdot \left(\frac{|\delta\underline{V}|}{|\underline{V}|} + \frac{|\delta\underline{M}|}{|\underline{M}|} \right) \quad (6)$$

where $|\underline{M}|$ is a norm of the matrix \underline{M} and $|\underline{V}|$ the corresponding norm of the vector \underline{V} . Any norm can be used but it may be advanta-

geous to use the smallest one, which is the euclidian norm of the vector \underline{V} :

$$|\underline{V}|_2 = \sqrt{(\sum_i v_i^2)} \quad (7)$$

and the corresponding spectral norm for the matrix \underline{M} :

$$|\underline{M}|_2 = \sqrt{\mu_1} \quad (8)$$

where μ_1 is the largest eigenvalue of $\underline{M}^H \underline{M}$, (\underline{M}^H being the hermitic conjugate of \underline{M}).

However, the following norms, which lead to faster calculations, are often used:

$$|\underline{V}|_1 = \sum_i |v_i| \quad (9)$$

and the corresponding norm for the matrix \underline{M} :

$$|\underline{M}|_1 = \max (|\underline{M}_j|_1) \quad (10)$$

where \underline{M}_j are the column vectors of \underline{M} .

The number

$$\text{cond } \underline{M} = |\underline{M}| \cdot |\underline{M}^{-1}| \quad (11)$$

appearing in (6) is of prime importance here, since $|\delta \underline{M}| \cdot |\underline{M}^{-1}|$ is generally much smaller than 1. It is the condition number of the matrix \underline{M} , which multiplies the experimental errors and transmits these errors into the result \underline{A} . This number depends only on the ex-

perimental design and on the model chosen. It can thus be calculated before making any experiment and constitutes a second (and even better) criterion for the choice of the experimental design.

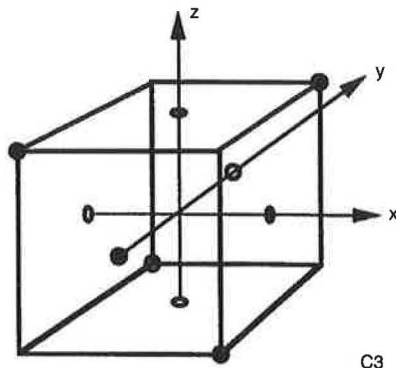
Examples of Experimental Designs

Several experimental designs were examined with the aim of mapping a 3-D cube with 10 measurements. The models tested were those of Equations 1 and 2 plus an interaction model which is Equation 2 without the square terms.

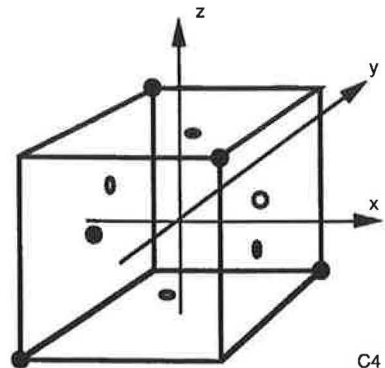
Several of these designs were found to be unusable (singular effect matrix or too large condition number for the quadratic model). The remaining designs are the following:

C3 has 6 points in the centre of the faces and 4 points at opposite corners. It was obtained by selecting 10 points out of the 27 points of a three-level factorial¹ design in such a way that the matrix \underline{M} receives the lowest condition number (Figure 1). The same result is obtained starting from the 125 points of a 5-level factorial design.

Fig. 1
Experimental
designs C3 (left)
and C4 (right).



C3



C4

¹ A k-dimensional, n-level factorial design is obtained by dividing the experimental domain (e.g. the interval [-1, 1]) on each axis into n equidistant levels. The complete factorial design contains all the points obtained by the n^k combination of the n possible values of the coordinates.

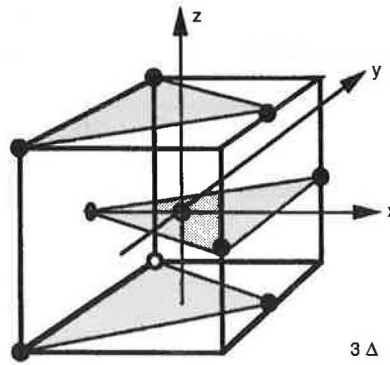
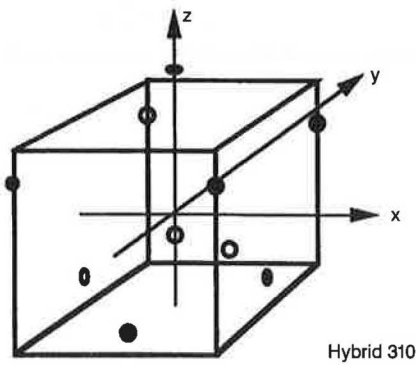


Fig. 2 Hybrid (left) and 3 Δ (right) experimental designs.

C4 has 6 points near the centre of the faces and 4 points at opposite corners. It was obtained by selecting 10 points out of the 65 points of a four-level factorial design which present the lowest condition number for the matrix \underline{M} .

The hybrid design has two points on the z-axis ($z = -0.136$ and $z = 1.2906$), four factorial points on the plane $z = 0.6386$ and a star-design in the plane $z = -0.9273$. Since there are points at locations larger than 1, all the coordinates should be divided by 1.2906 (Figure 2).

The 3 Δ design is made with points at the summits of 3 triangles placed at levels $z = -1$, 0 and 1, the middle one being in the opposite direction. The 10th point is at the centre of the zone.

The Hoke D2 and the Rechtschaffner design both have 7 points at the summits of the cube and 3 points at the centre of faces, but

the position of these last three points with respect to the others differs strongly (Figure 3). These designs were found in the literature (Feneuille et al., 1989) and chosen among others for having 10 measurement points.

The condition numbers of $\underline{M}'\underline{M}$ calculated according to Equations 10 and 11 for these designs and three models are given in Table 1.

Table 1 Condition numbers of $\underline{M}'\underline{M}$ for some experimental designs and three models. For each model, the best values are in bold characters and the worst in italics.

Experimental design	Quadratic model	Interactions model	Linear model
C3	4.33	3.15	1.00
C4	6.67	2.62	1.15
Hybrid 310	6.70	1.00	1.00
3Δ	8.88	1.414	1.11
Hoke D2	7.29	<i>3.19</i>	<i>1.66</i>
Rechtschaffner	9.24	2.03	1.23

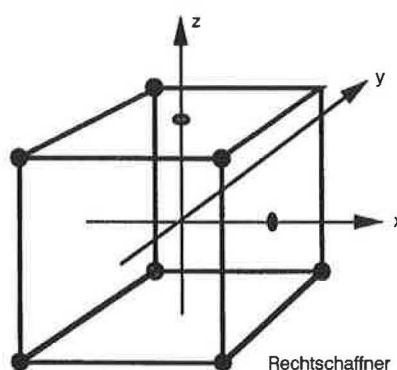
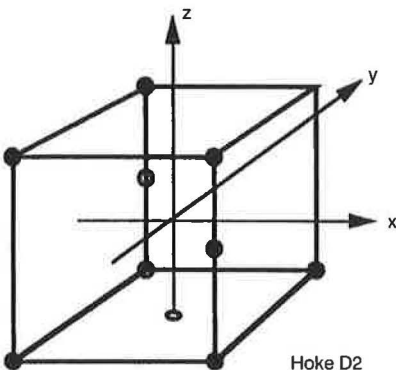


Fig. 3 Hoke D2 (left) and Rechtschaffner (right) experimental designs.

The three latter designs lead to a large condition number for a quadratic model, that is to large errors in the estimates of the coefficients. C 3 seems to be best if the model is quadratic or linear, while the hybrid and 3 triangles are better for interactions and linear models. However, the hybrid model does not map the whole domain and looks very asymmetric.

The designs recommended are C 3 if the quadratic or linear model is used and 3D for interaction or linear model.

It may also be interesting to draw the map of a contaminant (e.g. the CO₂) in the flat volume where the heads of the occupants are located. In this case, a two-dimensional design may be used. With a limited number of sampling points, the following designs may be recommended:

A 2-D full factorial design with 3 levels:

$$\begin{array}{r} X = \\ Y = \end{array} \quad \begin{array}{cccccccc} -1 & 0 & 1 & -1 & 0 & 1 & -1 & 0 & 1 \\ -1 & -1 & -1 & 0 & 0 & 0 & 1 & 1 & 1 \end{array}$$

which gives a condition number of 4.39 for a quadratic model. If 10 points are desired, adding (-0.5, 0) and (0.5, 0) lowers the condition number to 3.48. The minimum number of experiments is 6 for a quadratic model. The design:

$$\begin{array}{r} X = \\ Y = \end{array} \quad \begin{array}{cccccc} -1 & 1 & -1 & 0 & 1 & -1 \\ -1 & -1 & 0 & 0 & 0 & 1 \end{array}$$

has a condition number of 6.

For an interaction model, a recommended design is:

$$\begin{array}{r} X = \\ Y = \end{array} \quad \begin{array}{cccc} -1 & 1 & 0 & 1 & -1 \\ -1 & -1 & 0 & 1 & 1 \end{array}$$

which is also best for a linear model, even when the point (0,0) is removed. These designs have a condition number of 1, which is an absolute minimum.

Mapping the Concentration of a Contaminant

If the characteristics of the "natural" contaminant source(s) are known, they can be simulated either by the contaminant itself if it is easily analysed for non-toxic concentrations (such as CO₂ or H₂O) or by the injection of tracers at appropriate flow rates at the same locations.

The air is sampled at regular intervals at the locations corresponding to the experimental design and analysed. For each sampling time, or if the air- and contaminant-flow patterns are in steady state, a model is fitted to these points to estimate its parameters.

Once the parameters are estimated, the model can be used to find the probable location of a minimum or maximum concentration, to estimate the average concentration or the total amount of contaminant within the room.

The ventilation efficiency, also called the pollutant removal effectiveness, is generally defined as the ratio of two net concentrations:

$$\varepsilon_C = \frac{C_e - C_0}{C_x - C_0} \quad (12)$$

where:

C_e is the contaminant concentration in the exhaust air

C_0 is the contaminant concentration in the outdoor air

C_x is the contaminant concentration of interest.

The concentration of interest may be the concentration at a particular location in the room, the maximum concentration or the average of the whole room. Depending on that definition, different efficiencies may be defined and measured.

It is obvious that from the map of the concentration C_x and the measurement of the exhaust concentration C_e , a map of the ventilation efficiencies can be obtained, as well as

The experimental chamber

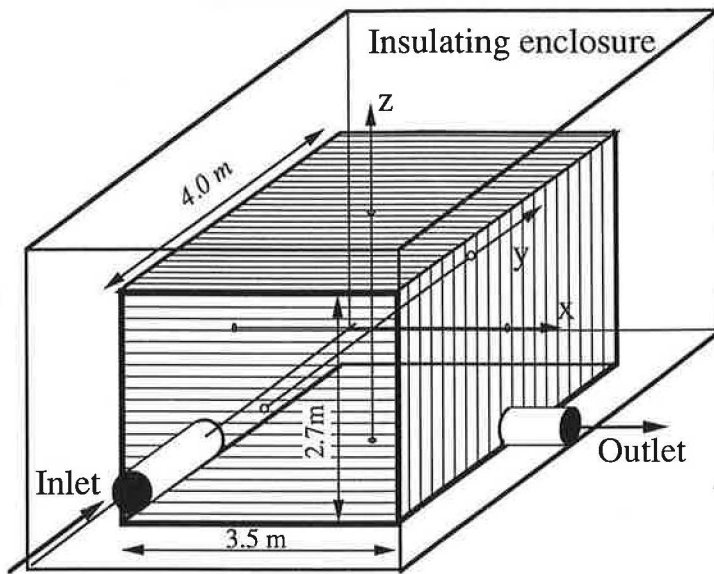


Fig. 4 The experimental chamber CHEOPS, with the inlet and outlet used for the present experiment.

any other value as maximum, average or minimum efficiency, assuming that the air leaves the room through a single exhaust duct.

When a first map is obtained, a “zoom” experiment may follow to obtain further details of an interesting part of the space. This experiment may use the same design but for a smaller volume.

Age of the Air

The particles of air coming from outside or from the ventilation system arrive at a given location in a room after a time τ which varies from one particle to the other. τ is called the age of the particle, as if it were born when entering the room.

Since there are a large number of air particles, a probability density $f(\tau)$ that the age of particles arriving at a given location is between τ and $\tau + d\tau$ and a probability $F(\tau)$ that this age is smaller than τ can be defined. It is shown that these probability functions can be measured by registering the concentration $C(\tau)$ of a tracer versus time, this tracer being either at uniform concentration at the beginning of the experiment, or injected at a con-

stant rate or as a short pulse at a single air inlet (Sandberg and Sjöberg, 1982; Shutcliffe, 1990).

The mean age of air at a given location in the room can be deduced from these distributions. The convenient formulas to be used are found in the literature (Shutcliffe, 1990). If, as was done in our experiments, the age is deduced from the decay in concentration of a tracer initially distributed in the room, the local mean age is calculated from:

$$\tau(\mathbf{r}) = \frac{\int_0^{\infty} C(\mathbf{r}, t) dt}{C(0)} \quad (13)$$

The average of the local mean age of air over the whole room is the room mean age $\langle \tau \rangle$. If the air leaves the room through a unique opening or duct, this room mean age can also be measured with tracer gas. The methods of injection are the same as before but the concentration $C_e(t)$ is measured in the exhaust duct. The room mean age is evaluated using Equation 15 below. If, as is often the case, the air leaves the room through multiple openings, leaks and outlets, the technique mentioned above cannot be used. However, the local age of air $\tau(\mathbf{r})$ can be

measured and mapped as well as a concentration, using the same experimental design. The average of the local mean age of air over the whole room is the room mean age of air $\langle \tau \rangle$.

Measurements

The Experimental Chamber

In order to evaluate the feasibility of the method presented above, measurements were performed in a well controlled room called CHEOPS ("CHambre Expérimentale d'Observation de Phénomènes de Stratification") (Figure 4). The room has airtight, lightweight walls, floor and ceiling. Its internal dimensions are 3.5×4.0 m with a height of 2.7 m; its volume is hence 37.8 m^3 . It is completely contained in a second enclosure measuring $5 \times 6 \times 4$ m, which is made of panes plated with 10 cm polystyrene foam, in order to control the temperature and temperature gradients within the internal room.

For this particular experiment, inlet and outlet openings were located in two walls, as shown in Figure 4. The airtightness of the room with closed openings was measured and found to be so high that airflows through parasitic leaks can be neglected when compared to the main airflow.

The Experiments

Before the experiments, the ends of 10 sampling tubes were fixed at 10 different locations

according to the two selected experimental designs, namely C3 and 3A. The other ends of these tubes were connected to a sampling scanner allowing sequential analysis of the air samples coming from these 10 locations. The analyser was a Binos from Leybold Heraeus and the tracer was N_2O .

During the experiments, an airflow rate of $18.9 \text{ m}^3/\text{h}$ (which corresponds to an air change of 0.5/h or a nominal time constant of 2 hours) was injected at the inlet. The airflow rate was controlled by both an airflow meter and tracer gas (constant concentration) techniques.

Since points near the walls do not represent the inner volume, the sampling points for the measurements were actually located, according to the experimental design, within a rectangular box smaller than the room itself, in such a way that there was a minimum distance of 50 cm between any sampling point and a wall, floor or ceiling.

After stabilization of the airflow and of the concentration, that is after about 4 hours, the tracer injection was stopped and the decay of the concentration was measured at 10 different locations according to the two selected experimental plans (Figure 5). The scanning interval between two channels was 42 seconds, so the time period between two measurements at the same location was 420 s or 7 minutes.

From these 10 decay curves, the local mean ages of air were deduced using

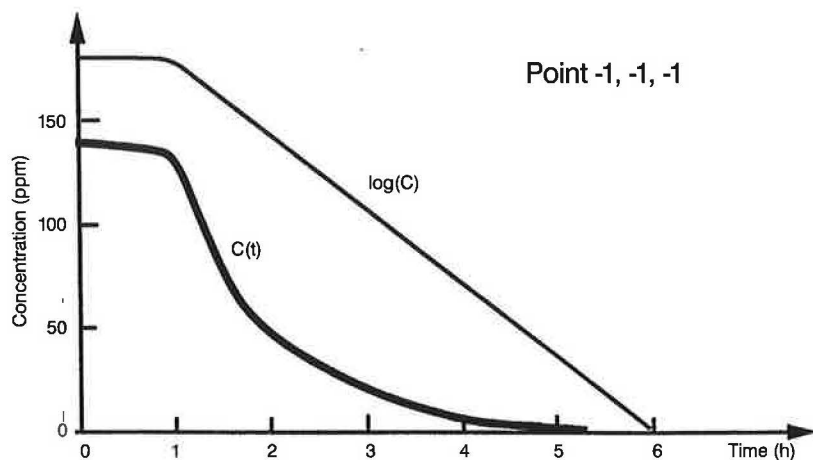


Fig. 5 Record of the concentration versus time (full line) at one location in the room, after cutting off the tracer injection. The dotted line shows the log of the concentration on an arbitrary scale. Note that the decay starts nearly one hour after the tracer injection stops.

Equation 13. These results are reported in Table 2, for two experiments with two different designs.

Table 2 Ages of air in the CHEOPS chamber for two experiments. The coordinates are given in units corresponding to the half dimensions of the chamber. The air outlet is at 1, 0, -1 and the inlet at -0.5, -1, 0.

x	y	z	3Δ	C3
-1	-1	-1	1.43	1.86
0	0	-1		1.83
1	0	-1	2.16	
-1	1	-1	1.41	
1	1	-1		1.56
0	-1	0		1.05
1	-1	0	1.02	
-1	0	0	1.09	1.06
1	0	0		0.99
0	0	0	1.06	
0	1	0		1.08
1	1	0	1.02	
-1	-1	1	0.94	
1	-1	1		0.98
0	0	1		0.99
1	0	1	1.00	
-1	1	1	0.96	0.96
Average of the ages (eq. 16)			1.209	1.236

First a quadratic model (Equation 2) was evaluated for these data for both experiments. Since the coefficients of the y, xy and yz terms were very small, a limited model was also tested, using:

$$\tau(r) = a + b_x x + b_z z + b_{xz} x z + b_{xx} x^2 + b_{yy} y^2 + b_{zz} z^2 \quad (14)$$

Table 3 gives the coefficients of these two models and the room mean ages obtained by different methods.

One of the measurement points in design 3Δ is located at the air outlet. The room mean age of air can hence also be measured using:

$$\langle \tau \rangle = \frac{\int_0^\infty t C_e(t) dt}{\int_0^\infty C_e(t) dt} \quad (15)$$

where $C_e(t)$ is the tracer concentration in the

only air outlet of the room. This value can be compared with the other values obtained either by the direct average of the measurements of the local mean ages:

$$\langle \tau \rangle = \frac{1}{N} \sum_i \tau_i(r_i) \quad (16)$$

or by the average of the map obtained: if a linear or interaction model is used, the room mean age of air is simply the constant term of the model. If a quadratic model is used, then:

$$\langle \tau \rangle = a + \frac{2}{3} \sum_i b_{ii} \quad (17)$$

where a is the constant term of the model and b_{ii} are the coefficients of the square terms.

Table 3 Coefficients of two models calculated from measurements made under similar conditions but with two different experimental designs. The coefficients which are very small in the quadratic model are put to zero in the limited model.

Model	Quadratic		Limited	
	3Δ	C3	3Δ	C3
Constant	1.06	1.08	1.06	1.08
X	0.08125	-0.03	0.08125	-0.0583
Y	0	0.01		
Z	-0.4075	-0.42	-0.4075	-0.3867
X*Y	0	-0.05		
X*Z	-0.1725	0.09	-0.1725	0.08
Y*Z	0.01	0.03		
X ²	0.1112	-0.055	0.1112	-0.055
Y ²	-0.2325	-0.015	-0.2325	-0.015
Z ²	0.3275	0.33	0.3275	0.33
Mean age (eq. 17)	1.197	1.253	1.197	1.253
Room mean age measured at the outlet (eq. 15, 3Δ design): 1.21 h				

A map of the local mean age of air can be drawn using the model, as shown in Figure 6.

Finally, the air change efficiency, which expresses how quickly the air in the room is replaced, is calculated by:

$$\varepsilon = \frac{\tau_n}{2\langle\tau\rangle} = \frac{2}{2.4} = 0.83 \quad (18)$$

where $\langle\tau\rangle$ is the room mean age of air and τ_n is the nominal time constant of the room. This efficiency is 1 for piston ventilation and 0.5 for complete mixing.

Discussion and Conclusions

Comparison of the results in Table 2 show that:

- (1) as expected, there are important differences (up to a factor of 2) in the age of air at different locations; it confirms that either a strong mixing or sampling at several places is necessary to measure the air change rate or the nominal time constant of the room with tracer gas techniques;
- (2) there are slight differences between the two experiments, as can be seen by the values marked in bold characters, which are measured at the same locations. This effect is particularly high at the point -1, -1, -1. Even when the experiment is performed under very similar conditions, small changes in air temperatures may affect the flow pattern.

As shown in Table 3, the coefficients of the model obtained with two different designs do not differ much. Moreover, the room mean ages obtained by various means from the measurements are very close. This value is affected neither by small changes in air temperature nor by the experimental planning, as long as it is good. Note that the good agreement between the ages of air measured at the exhaust and averaged within the room does not mean much for the accuracy of the mapping.

Hence, if there is not a single air outlet, or *a fortiori* when the air outlets cannot be clearly identified, the room mean age of air may be obtained by averaging several measure-

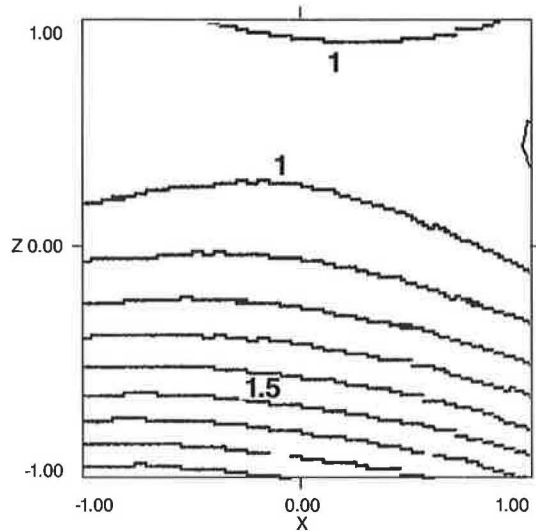


Fig. 6: Lines of constant age of air in the plane $y = 0$ drawn with the limited model adjusted to the measurements made with the C3 design. The younger air is at the top of the zone even with the inlet at the mid-plane.

ments taken at convenient locations. It is safer, however, to deduce it from the coefficients of a fitted model.

Finally, it is shown that, if the experiments are well designed, it is possible to draw a map either of the concentration of a contaminant and the related quantities as the ventilation efficiency or of the local mean age of air, with a reasonable number of measurements. These maps also allow the fresh or contaminant flows as well as the ventilated and stagnant zones to be deduced.

However, clear details cannot be reproduced with a limited number of measurement points. This is the case in the distribution of the age of air (or of the contaminant concentration) near the fresh air inlet (or the contaminant source). If the number of measurement points is limited, these few measurements can be used to calibrate a simulation with a sophisticated code (e.g. Phoenics) at these locations. The code is then used to interpolate correctly between the measurements and more confidence is gained in the description of the details.

If the possible number of measurement

locations is large, mapping could be performed with clearer details. However, one could take advantage of the method presented above to choose, among several possible sampling networks, the one leading to the most accurate results.

Finally, any prior knowledge of the quantity to be mapped should be used in the planning of the experiment. For example, if the concentration of a contaminant is to be mapped only in the occupied space, the experimental zone should be restricted to that space. Or, if it is actually known that the air moves in one direction only (piston-type ventilation), the sampling locations could be on a straight line in that direction.

Acknowledgements

This research was sponsored by the NEFF ("Nationaler Energie-Forschungs-Fonds" or

National Energy Research Funds). The codes NEMROD from LPRAI, Marseille and XSTAT (John Wiley and Sons) were used to design and analyse the experiments.

References

- Bandemer, H. and Bellmann, A. (1979) *Statistische Versuchsplanung*. BSB G. Leipzig, Teubner Verlag.
- Bevinton, Ph. (1969) *Data Reduction and Error Analysis for the Physical Sciences*, New York, McGraw Hill.
- Davidson, L. and Olsson, E. (1987) "Calculation of age and local purging flow rate in rooms", *Building and Environment* 22, 111-127.
- Feneuille, D., Mathieu, D. and Phan-Tan-Luu, R. (1989) *Méthodologie de la recherche expérimentale*, Marseille, Cours IPSOI, R. H. Poincaré.
- Sandberg, M. and Sjöberg, M. (1982) "The use of moments for assessing air quality in ventilated rooms", *Building and Environment*, 18, 181-197.
- Shutcliffe, H. (1990) *A Guide to Air Change Efficiency*, Bracknell, (AIVC technical note 28).
- Valton, P. (1989) "Renouvellement d'air dans les bâtiments", *PROMOCLIM E*, 18(5), 279-297.